





Improvement of Neurological Function in Rats with Ischemic Stroke by Adipose-derived Pericytes

Cell Transplantation
Volume 29: 1–12
© The Author(s) 2020
Article reuse guidelines:
sagepub.com/journals-permissions
DOI: 10.1177/0963689720956956
journals.sagepub.com/home/cll


Vyacheslav Ogay¹ , Venera Kumasheva¹, Yelena Li¹,
Sholpan Mukhlis¹, Aliya Sekenova¹, Farkhad Olzhayev²,
Andrey Tsoy², Baurzhan Umbayev², Sholpan Askarova² ,
Azat Shpekov³, Assylbek Kaliyev⁴, Berik Zhetpisbayev⁴ ,
Yerbol Makhambetov⁴, Serik Akshulakov⁴, Arman Saparov⁵,
and Yerlan Ramankulov^{1,6}

Abstract

Pericytes possess high multipotent features and cell plasticity, and produce angiogenic and neurotrophic factors that indicate their high regenerative potential. The aim of this study was to investigate whether transplantation of adipose-derived pericytes can improve functional recovery and neurovascular plasticity after ischemic stroke in rats. Rat adipose-derived pericytes were isolated from subcutaneous adipose tissue by fluorescence-activated cell sorting. Adult male Wistar rats were subjected to 90 min of middle cerebral artery occlusion followed by intravenous injection of rat adipose-derived pericytes 24 h later. Functional recovery evaluations were performed at 1, 7, 14, and 28 days after injection of rat adipose-derived pericytes. Angiogenesis and neurogenesis were examined in rat brains using immunohistochemistry. It was observed that intravenous injection of adipose-derived pericytes significantly improved recovery of neurological function in rats with stroke compared to phosphate-buffered saline-treated controls. Immunohistochemical analysis revealed that the number of blood capillaries was significantly increased along the ischemic boundary zone of the cortex and striatum in stroke rats treated with adipose-derived pericytes. In addition, treatment with adipose-derived pericytes increased the number of doublecortin positive neuroblasts. Our data suggest that transplantation of adipose-derived pericytes can significantly improve the neurologic status and contribute to neurovascular remodeling in rats after ischemic stroke. These data provide a new insight for future cell therapies that aim to treat ischemic stroke patients.

Keywords

pericytes, neurogenesis, angiogenesis, neurological recovery, ischemic stroke

Introduction

Stroke is one of the most common cardiovascular diseases in the world¹. According to the latest data from the World

Health Organization, it has the second highest mortality rate after coronary heart disease and is the first leading cause of persistent disability of population². Currently, thrombolytic

¹ Stem Cell Laboratory, National Center for Biotechnology, Nur-Sultan, Kazakhstan

² National Laboratory Astana, Nazarbayev University, Nur-Sultan, Kazakhstan

³ Department of Neurosurgery, Medical Centre Hospital of the President's Affairs Administration of the Republic of Kazakhstan, Nur-Sultan, Kazakhstan

⁴ Vascular and Functional Neurosurgery Department, National Center for Neurosurgery, Nur-Sultan, Kazakhstan

⁵ School of Medicine, Nazarbayev University, Nur-Sultan, Kazakhstan

⁶ School of Science and Technology, Nazarbayev University, Nur-Sultan, Kazakhstan

Submitted: July 4, 2020. Revised: August 13, 2020. Accepted: August 18, 2020.

Corresponding Author:

Vyacheslav Ogay, Stem Cell Laboratory, National Center for Biotechnology, Korgalzhyn Highway 13/5, Nur-Sultan 010000, Kazakhstan.

Email: ogay@biocenter.kz



Creative Commons Non Commercial CC BY-NC: This article is distributed under the terms of the Creative Commons Attribution-NonCommercial 4.0 License (<https://creativecommons.org/licenses/by-nc/4.0/>) which permits non-commercial use, reproduction and distribution of the work without further permission provided the original work is attributed as specified on the SAGE and Open Access pages (<https://us.sagepub.com/en-us/nam/open-access-at-sage/>).

therapy is used for ischemic stroke treatment, which allows for the restoration of blood flow in the affected vessel and the prevention of irreversible changes in the brain tissue. Among all kinds of medicinal and mechanical methods used for vessel recanalization, the largest and most convincing evidence-based treatment of patients with ischemic stroke is systemic thrombolysis using recombinant tissue activator of plasminogen (rt-PA) performed in the first 4.5 h after the onset of stroke symptoms³. However, as shown by clinical practice, the use of rt-PA therapy has limitations related to the narrow “therapeutic window” and high rate of symptomatic intracerebral hemorrhage, exacerbating the consequences in poststroke patients⁴. In this regard, only 5% of the patients could benefit from rt-PA therapy. For the majority of stroke patients, the therapy that used the drugs for blood flow restoration in the ischemic area and maintained the brain tissue metabolism was shown to be inefficient⁵.

As an alternative to thrombolytic therapy, the development of cell-based restorative approaches is promising for the treatment of stroke^{6,7}. A number of preclinical and clinical studies showed that cell-based therapy with mesenchymal stem cells (MSCs) isolated from different tissues and organs improves neuroplasticity and neurological outcome through the upregulation of restorative processes such as neurogenesis, angiogenesis, and oligodendrogenesis after ischemic stroke⁸⁻¹⁰. Recently, besides MSCs, the therapeutic potential of pericytes has attracted great interest in regenerative medicine^{11,12}.

Pericytes are a rare heterogeneous population of multipotent progenitor cells that can be isolated from various vascularized tissues and organs of humans and animals [bone marrow, adipose tissue (AT), brain, skeletal muscle, liver, and placenta]^{13,14}. Pericytes attracted the attention of scientists and clinicians due to their multilineage differentiation potential and active participation in the restoration and regeneration of tissues after injury¹⁵. When stimulated by appropriate factors, pericytes are able to differentiate into a number of specialized cell types, such as adipocytes, chondrocytes, osteoblasts, endothelial cells, neurons, astrocytes, and oligodendrocytes¹⁶⁻¹⁸. Moreover, pericytes can produce neurotrophic and angiogenic growth factors, which indicates their regenerative and neuroprotective properties¹⁹. Pericytes surrounding the blood vessels of the brain constantly express nestin—a marker of neuronal progenitor cells and hence, may be involved in neuronal regeneration¹⁸. Indeed, it was recently shown that pericytes play an important role in repairing the nervous tissue during cerebral ischemia, as they can differentiate into neurons and glial cells in the hippocampal subgranular zone of monkeys²⁰. Moreover, pericytes can induce endothelial cells to form tube-like structures, as well as promote angiogenesis¹⁴. Dar et al. demonstrated that transplantation of pericytes increased the formation of new vessels and improved blood flow in the murine ischemic limb model²¹. Furthermore, it was shown that human pericytes isolated from skeletal muscles render regenerative effects in coronary heart diseases, such as improvement of

angiogenesis, scar reduction, and suppression of chronic inflammation due to the possible secretion of various trophic factors²². Thus, based on this evidence, we have come to the idea of investigating whether intravenous (IV) administration of adipose-derived pericytes (ADPs) can improve functional recovery and neurovascular plasticity in a rat model of focal cerebral ischemia. The choice of AT as a source of pericytes was determined for the following reasons: (1) easy availability and simple sampling of AT for isolating of perivascular cells and (2) AT contains approximately 15% pericytes, whereas adult bone marrow contains less than 0.5% pericytes of the total mononuclear cells²³. In addition, in the present study, we have revealed the optimal amount of ADP transplantation to exert a significant therapeutic effect on the improvement of neurological function and enhancement of endogenous angiogenesis and neurogenesis in ischemic stroke rats.

Materials and Methods

Animals

Male Wistar rats 10–12 weeks old were purchased from Laboratory Animal Company “Pushchino” (Pushchino, Moscow region, Russia). The animals were housed in a temperature-controlled environment (23°C) with 60% relative humidity applying a 12 h light/dark cycle. The animals had ad libitum access to food and water. Experimental procedures involving animals were in full compliance with current international laws and policies (Guide for the Care and Use of Laboratory Animals, National Academy Press, 1996) and were approved by the Local Ethics Committee for Animal Use in National Center for Biotechnology.

Isolation and Culture of ADPs

For the isolation of pericytes, subcutaneous AT from the Wistar rats was isolated and washed three times with phosphate-buffered saline (PBS) containing 200 U/ml penicillin, 200 µg/ml streptomycin, and 50 µg/ml amphotericin B to remove the red blood cells. After washing, the AT was transferred into a Petri dish and cut into small pieces with a scalpel. Next, the AT was digested in 0.25% collagenase Type I (Gibco, Grand Island, NY, USA) at 37°C on a shaker for 60 min. After centrifugation, the pellets were resuspended in complete growth medium [Alpha Modified Eagle’s Medium, 10% fetal bovine serum (FBS), 1% penicillin/streptomycin/amphotericin B] and filtered through a 40-µm cell strainer. Obtained cell suspension was directly used for fluorescence-activated cell sorting (FACS Aria III, BD Biosciences, San Jose, CA, USA).

Afterward, the cells were resuspended in blocking buffer (PBS, 0.5% bovine serum albumin, 2 mmol/l ethylenediaminetetraacetic acid) at a concentration of 5×10^6 cells/ml prior to incubation with the following antibodies: CD146-Alexa Fluor 488 (dilution 1:50, clone EPR3208, Abcam, Cambridge, UK; ab196448) and CD34-PE (dilution 1:100,

clone EP373Y, Abcam; ab223930), rabbit IgG PE isotype control (dilution 1:100, clone 60024B, R&D Systems, Minneapolis, MN, USA, IC1051P) and rabbit IgG Alexa Fluor® 488 isotype control (dilution 1:100, clone EPR25A, Abcam; ab199091). The cells were incubated with the antibodies for 30 min at 4°C, then washed with PBS, centrifuged, and resuspended in α -MEM (Gibco) containing 20% FBS. In order to avoid aggregation of the cells during the sorting, DNase I (100 mg/ml with 5 mM MgCl₂) was added. CD146⁺CD34⁻ cells were collected in the 15 ml collection tube containing 5 ml of α -MEM, 20% FBS, 1% penicillin, and streptomycin.

After sorting, CD146⁺CD34⁻ cells were transferred into a complete growth medium and plated in culture flasks for culture and expansion at 37°C in an incubator with 5% CO₂. After 3 days of incubation, the culture flasks were washed with PBS to remove nonadherent cells and kept in a complete growth medium. The culture medium was changed every 2 days. When the cells reached 70%–80% confluence, the cells were harvested using TrypLE Express (Gibco), counted, and split into new culture flasks.

Immunocytochemistry

The ADPs (passage 3) were grown on a four-well chambered cell culture slide. After fixation with 4% paraformaldehyde and washing with PBS, the cells were incubated with primary antibody against CD146 (dilution 1:100; ab210072), PDGFR- β (dilution 1:100; ab69506), NG2 (dilution 1:100; ab50009), CD45 (dilution 1:100; ab10558), CD34 (dilution 1:100; ab81289), CD31 (dilution 1:100; ab119339), CD73 (dilution 1:100; ab175396), CD90 (dilution 1:100; ab225), CD105 (dilution 1:100; ab11414), Nestin (dilution 1:100; ab11306), and MAP2 (dilution 1:100; ab36447) (all from Abcam, see Supplemental Table 1) in PBS/0.1% Tween 20 and 10% normal goat serum overnight at 4°C. The cells were washed with PBS and incubated with secondary antibodies: goat anti-rabbit IgG Alexa Fluor 594 (dilution 1:500; A-11012), goat anti-rabbit IgG Alexa Fluor 488 (dilution 1:500; A-11008), and goat anti-mouse IgG Alexa Fluor 488 (dilution 1:500; A-11029) (all from Thermo Fisher Scientific, Waltham, MA, USA) in PBS for 45 min at room temperature. After washing in PBS, the cells were mounted in antifade reagent with 4',6-diamidino-2-phenylindole (DAPI; Thermo Fisher Scientific) for 1 min and visualized with an inverted fluorescence microscope Axio Observer A1 (Carl Zeiss, Jena, Germany).

Colony-forming Unit-fibroblast Assay

The ADPs (passage 3) were harvested using TrypLE Express, and the total cell number was determined by using an automatic cell counter BioRad TC20. Harvested cells were seeded into culture flasks at a density of 250 cells, 500 cells, and 1,000 cells. After 14 days, cell cultures were washed with PBS and stained with 0.5% Crystal Violet in

methanol for 10 min at room temperature. After staining, flasks were washed with PBS, allowed to dry, and colonies were counted and analyzed by using a stereomicroscope SZ61 (Olympus, Hamburg, Germany).

Multilineage Differentiation Assay

For adipogenic differentiation, 1×10^4 cells/cm² were plated in a six-well culture plate and cultivated in an adipogenic differentiation medium composed of high-glucose Dulbecco's modified Eagle's medium (DMEM) supplemented with 15% FBS, 0.2 mM L-glutamine, 100 μ M L-ascorbic acid, 200 μ M indomethacin, and 100 nM dexamethasone. The medium was changed twice a week. After 21 days, the cells were fixed with 4% paraformaldehyde and stained with Oil Red O.

For osteogenic differentiation, the cells at 90% confluence were cultivated in an osteogenic differentiation medium composed of low glucose DMEM supplemented with 15% FBS, 200 μ M L-ascorbic acid, 10 mM glycerolphosphate, and 100 nM dexamethasone. The medium was changed twice a week for 3 weeks. Osteogenic differentiation was evaluated using Alizarin Red staining.

For chondrogenic differentiation, the cells were resuspended at 1.25×10^6 cells/ml in a chondrogenic differentiation medium composed of high-glucose DMEM supplemented with 1% ITS + Premix, 100 μ mol/l ascorbate-2-phosphate, 0.1 μ M dexamethasone, and 10 ng/ml TGF- β 1. To create chondrogenic micromass pellets, 2.5×10^5 cells from this cell solution were placed in a 96-well polypropylene plate, centrifuged at 500 \times g, and placed in an incubator at 37°C and 5% CO₂. The medium was changed twice a week. After 3 weeks, the cell pellets were harvested, fixed with 10% neutral-buffered formalin, paraffin-embedded, sectioned at 5 μ m, and stained with toluidine blue.

For endothelial differentiation, 3×10^3 cells/cm² were first plated in a plastic petri dish and cultured in an endothelial growth medium EGM-2 (Lonza, Walkersville, MD, USA) for 10 days at 37°C and 5% CO₂. At 24 h, the cell culture was placed in a 3D mini-shaker (Biosan, Riga, Latvia) and rotated at a rate of 20 rpm. On day 10, the cells were reseeded at a density of 3×10^4 cells/cm² in the six-well plate covered by growth factor reduced Matrigel diluted 1:1 in EGM-2 without growth factors and cultured for 24 h. The formation of capillary-like structures was observed using an inverted microscope.

For neuronal differentiation, 1×10^4 cells/well were plated on a poly-L-lysine-coated four-well chambered cell culture slide and cultured in α -MEM supplemented with 15% FBS. After 3 days, the cell monolayer was washed three times with PBS. Then, the medium was replaced with DMEM/F12, containing N2 and B27 supplements. At 24 h after neuronal induction, the cells were fixed for immunocytochemistry.

Middle Cerebral Artery Occlusion Model

Adult male Wistar rats (280–330 g) were used for ischemic stroke experiments. The middle cerebral artery occlusion (MCAO) was carried out according to the intraluminal suture method²⁴. Briefly, under general anesthesia (1.5% isoflurane, anesthesia machine was set to 1.0 l/min O₂ and 1.0 l/min N₂O), the left common carotid artery, external carotid artery (ECA), and internal carotid artery were exposed. The occipital artery and superior thyroid artery branches off of the left ECA have been ligated and cut. ECA stump was tied up to hold the intraluminal suture in place. Next, the ECA was cut with a microscissor and a 4–0 monofilament nylon suture with silicone-coated tip (Doccol Corp., Redlands, CA, USA) was inserted through an arteriotomy of the left ECA into the left MCA. In order to prevent hypothermia during the surgery procedure, the body temperature of the rats was maintained at $37 \pm 2^\circ\text{C}$ using a heating blanket. Measurement of the core temperature of the animals during MCAO was performed with a digital rodent thermometer BIO-TK8851 (Bioseb Lab Instruments, Vitrolles, France). After MCAO for 90 min, the monofilament nylon suture was removed and the ECA was ligated with a 3–0 silk suture. In order to provide hydration during the recovery stage, 5 ml of prewarmed PBS was injected intraperitoneally into the rats. Twenty-four hours after MCAO, the animals were examined for any indications of functional deficiency by a simple behavior test previously described by Bederson et al²⁵. Evaluation of functional deficiency was performed by giving a score on a scale of 0–3. The animals with severe functional deficiency (grades 2 and 3) were included in the study.

IV Injection of ADPs

Rats with severe neurological deficits were divided into four experimental groups: the group received IV injection of PBS without Ca₂⁺ and Mg₂⁺ serves as control (PBS group, $n = 6$); the group received IV injection of 1×10^6 of ADPs (1 million ADPs group, $n = 6$); the group received IV injection of 3×10^6 of ADPs (3 million ADPs group, $n = 6$); the group received IV injection of 6×10^6 of ADPs (6 million ADPs group, $n = 6$). Before IV injection, rat ADPs (passage 5) were detached from T75 culture flasks by TrypLE Express. To avoid cell clumping, ADPs were washed twice by PBS without Ca₂⁺ and Mg₂⁺ and additionally filtered through 40 μm cell strainer (Corning Costar, Durham, NC, USA). Next, the cells were counted and resuspended in the following concentrations: 1×10^6 , 3×10^6 , and 6×10^6 cells in 0.3 ml of PBS without Ca₂⁺ and Mg₂⁺.

In order to perform IV injection, the rats (24 h after MCAO) were subjected to isoflurane anesthesia. Then tail vein from lateral side was dilated by warming using lamp. Injections of cell suspension (1×10^6 cells, 3×10^6 cells, and 6×10^6 cells in 0.3 ml PBS or 0.3 ml PBS alone) were performed manually by a syringe with 29-gauge needle. The needle was inserted at the upper 1/2 to 1/3 of the tail. Cell

suspension was injected slowly. After finishing injection, the needle was removed while pressing a part of puncture with the thumb to prevent leakage of the cell suspension. All procedures were performed under aseptic conditions.

Behavioral Tests

For functional recovery evaluation, a walking beam test²⁶ and a modified neurological severity score (mNSS) were performed. Animals were trained prior to MCAO, and deficits were evaluated at 1, 7, 14, and 28 days after IV injection of the cells. The observer was blinded to the experimental condition. The mNSS includes motor, sensory, reflex, and balance tests. The mNSS was used to evaluate the sensorimotor deficits by grading the score on a scale of 0–18 (see Supplemental Table 2).

Walking beam test was used to assess fine motor coordination and function. Briefly, rats were exposed to bright light and loud white noise, which they escaped by walking along a narrowed wooden beam (2.5×122.0 cm) and into a darkened goal box at the opposite end of the beam. The latency for the rat to reach the goal box (not to exceed 60 s) and hindlimb performance as the animal traversed the beam based on a 1–7 rating scale (1—unable to traverse beam and cannot place affected limbs on horizontal beam surface; 2—unable to traverse beam but places affected limbs on horizontal beam surface and maintains balance for ≥ 5 s; 3—traverses beam by dragging affected hindlimbs; 4—traverses beam and, at least once, places affected limbs on horizontal beam surface; 5—traverses beam successfully but uses affected limbs in $<50\%$ of steps along beam; 6—traverses beam successfully and uses affected limbs to aid $>50\%$ of steps along beam; and 7—traverses beam normally with both affected paws on horizontal beam surface, neither paw ever grasps the side surface, and there are no more than two footslips) were recorded. The testing process was recorded on a digital camera followed by the analysis of the number of slips of the limbs.

2,3,5-Triphenyltetrazolium Chloride Staining

To assess ischemic lesion after MCAO, the rats were scarified by euthanasia and the brains were carefully removed on ice. Then, the brains were frozen for 20 min at -20°C and sliced into 2-mm-thick consecutive sections. The sections were put in Petri dish containing 2% 2,3,5-triphenyltetrazolium chloride (TTC; Sigma-Aldrich, St. Louis, MO, USA) and incubated at 37°C for 20 min in the dark place. The TTC solution was then replaced with 10% buffered formalin. Infarcted zone and healthy tissues appeared white and red color, respectively. Brain sections were photographed using a digital camera EOS 550D (Canon Inc., Tokyo, Japan). The lesion volume was calculated as follows: (right hemisphere area – left uninfarcted area)/(right hemisphere area $\times 2$). The infarcted area was determined as a percentage of dead cerebral tissue.

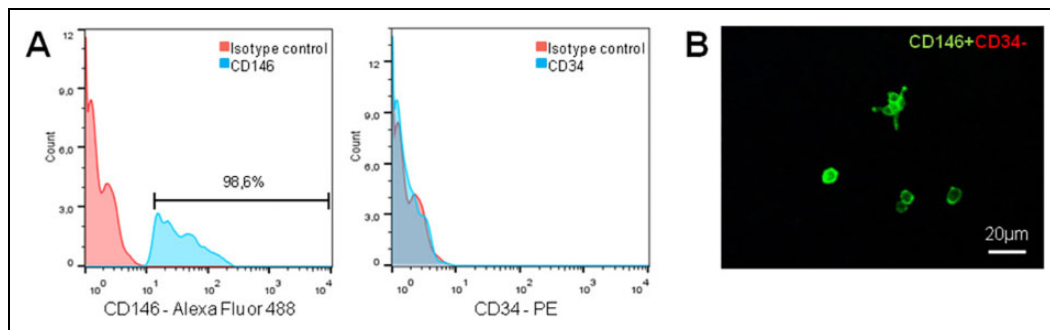


Figure 1. Gating strategy to isolate CD146⁺CD34⁻ pericytes from adipose tissue. After dissociation and filtering into a single cell suspension, cells were subjected to a FACS to isolate CD146⁺CD34⁻ pericytes. Live cells were selected by 7-AAD exclusion with a DUMP channel. Single cells with appropriate size were included in PI, and doublets, cell clumps, and debris were excluded by the SSC and FSC gates. (A) For separation of cell of interest, two-color sorting was used. The cells labeled with antibodies to CD146 and CD34 were sorted and CD146⁺CD34⁻ population was selected. During cell sorting only high fluorescence-stained cells were taken into account. Appropriate rabbit IgG-PE and IgG-Alexa Fluor 488 were used as isotype controls. (B) Representative image of isolated CD146⁺CD34⁻ ADPs (green fluorescence) after 4 h of incubation in a complete culture medium α -MEM supplemented with 10% FBS and 1% antibiotics. FACS: fluorescence-activated cell sorting; FBS: fetal bovine serum.

Histological Evaluation

In order to evaluate histopathological changes at 24 h after MCAO, rat brains were fixed in a 10% solution of neutral formalin after completion of the experiments. The samples were sequentially dehydrated in 70%, 95%, 95%, 100%, and 100% ethyl alcohol, after washing in phosphate buffer, then immersed in xylene. After that, the samples were infiltrated with paraffin and enclosed in paraffin blocks. Histological sections with 4 μ m thickness were cut on a microtome (Leica, Nussloch, Germany) and applied to a glass slide. The slides with paraffin sections were treated twice with xylene to remove paraffin. Then rehydration of samples was carried out according to the following scheme: 100%, 100%, 95%, 95%, 70% ethyl alcohol, and distilled water. Thereafter, the samples were stained with hematoxylin, washed with water, stained with eosin, and sequentially dehydrated with ethyl alcohol 95%, 95%, 100%, and 100%. Histological medium was applied to the slides and each slide was covered with a cover slip after processing with xylene. Analysis of the stained samples was carried out with a light microscope Axio Scope A1 (Carl Zeiss).

Lesion Volume Measurement and Immunohistochemistry

Before immunohistochemical analysis, 50 mg/kg of the 5-bromodeoxyuridine (BrdU) was injected intraperitoneally to rats daily starting 24 h after MCAO for 14 days to stain proliferated cells in the brain. All animals were sacrificed 4 weeks after ADPs administration by carbon dioxide euthanasia. The brains were carefully removed from the skull and fixed in 4% paraformaldehyde solution for 24 h at 4°C. Then, postfixed brains were transversally cut into two equal parts. One part of the brain was processed for immunohistochemistry, and another part of the brain was prepared for infarction volume measurement. For

immunohistochemistry, brain samples were immersed in 30% sucrose for 24 h, embedded in Tissue-Tek O.C.T. compound (Sakura Finetek, Torrence, CA, USA), and sectioned on a cryostat MNT (SLEE medical GmbH, Mainz, Germany). Afterward, sections were incubated with primary antibodies against CD31 (dilution 1:100; ab119339), BrdU (dilution 1:50; ab8152), and doublecortin (DCX, dilution 1:200; ab18723) (all from Abcam) for 1 h at 37°C in humidified chamber. After washing with PBS, sections were incubated with goat anti-mouse IgG Alexa Fluor 488 (dilution 1:500, Thermo Fisher Scientific; A-11029) and goat anti-rabbit IgG Alexa Fluor 594 (dilution 1:500, Thermo Fisher Scientific; A-11012) for 45 min at 37°C in the dark. Cell nuclei were stained with 1 μ g/ml DAPI (Thermo Fisher Scientific) for 5 min. After staining, the sections were mounted with antifade solution, covered by coverslip, and analyzed with fluorescence microscope Axio Scope A1 (Carl Zeiss). For infarction volume measurement, brain samples were infiltrated with 30% sucrose solution for 3 days, embedded in Tissue-Tek O.C.T. compound and sectioned in 10- μ m-thick slices, stained with hematoxylin and eosin (H&E), and coverslipped with DPX mounting medium (Sigma-Aldrich, St. Louis, MO, USA). Total brain, left hemisphere area, and injured area were analyzed with ImageJ software. Lesion volume was calculated using method previously described by Swanson et al²⁷.

Statistical Analysis

All data are presented as mean \pm standard deviation. The statistical significance was calculated using one-way analysis of variance with Bonferroni's multiple comparison tests. $P < 0.05$ was considered statistically significant. Statistical analysis was conducted with software Statistica 6.0 (Stat-Soft, Tulsa, OK, USA).

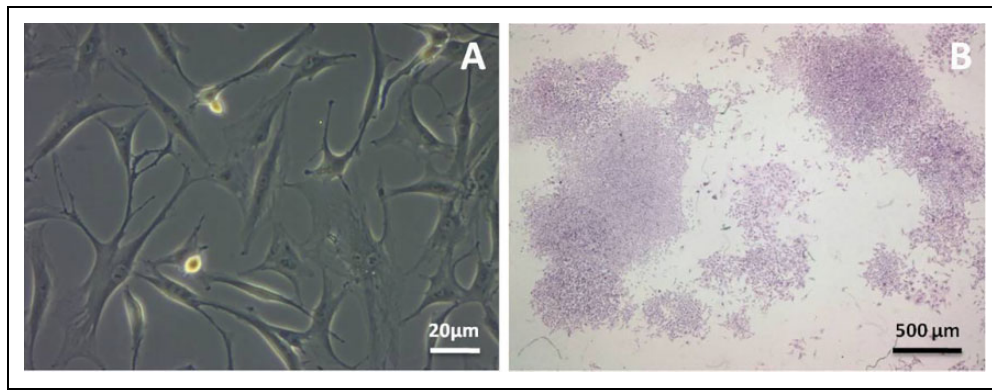


Figure 2. Morphology and clonogenic capacity of rat ADPs. (A) Phase-contrast image of live rat ADPs. (B) Rat ADPs form fibroblastic colonies. Crystal violet staining. ADPs: adipose-derived pericytes.

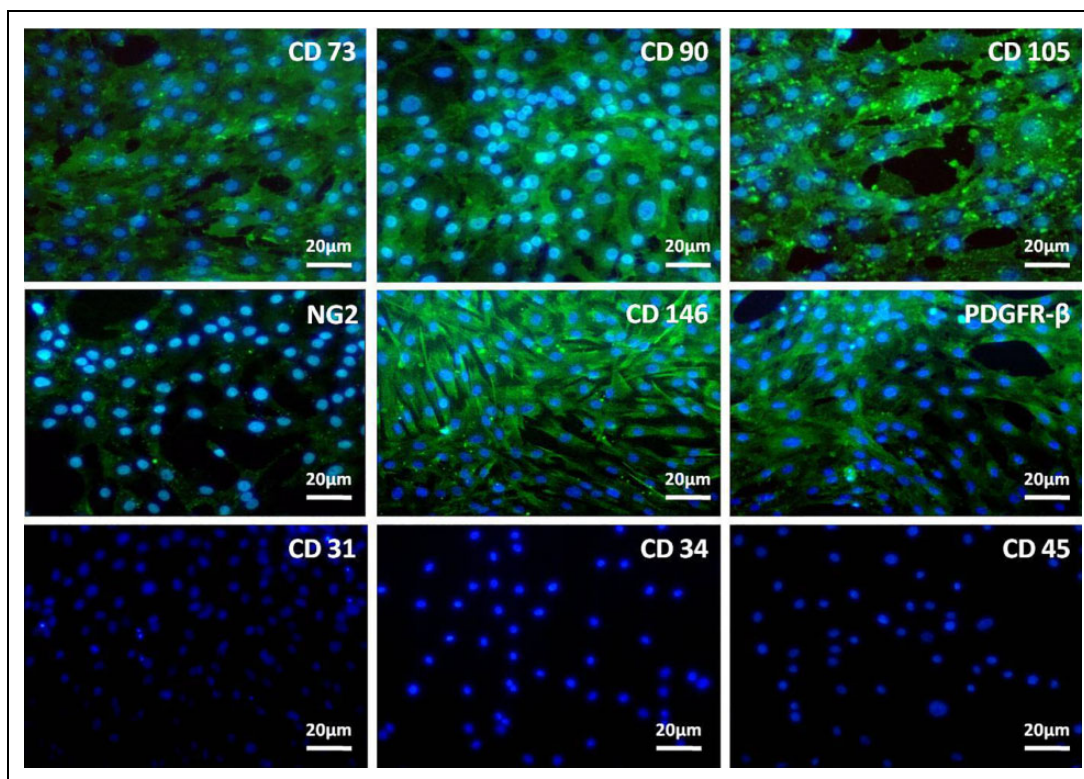


Figure 3. Immunofluorescence analysis of rat ADPs. The cells express both mesenchymal stem cell and pericyte-related markers (CD73, CD90, CD105, CD146, PDGFR- β , and NG2) but not endothelial and hematopoietic markers (CD31, CD34, and CD45). The nuclei are stained with DAPI. ADPs from passage 3 and passage 4 were used for this analysis. ADPs: adipose-derived pericytes; DAPI: 4',6-diamidino-2-phenylindole.

Results

In order to isolate rat ADPs, we used the antibody to CD146 (a surface marker of pericytes and endothelial cells) and antibody to CD34 (a surface marker of hematopoietic and endothelial cells). For isolation of ADPs, only the cells with a phenotype CD146⁺CD34⁻ were considered. The results of FACS cell sorting of CD146⁺CD34⁻ cells from rat AT are shown in Fig. 1A. Purified ADPs were positive for CD146 expression (98.6%) and negative for a CD34

marker. Next, sorted CD146⁺CD34⁻ cells were resuspended in a complete culture medium and expanded for further characterization. A short-term culture of purified ADPs is shown in Fig. 1B.

Rat ADPs were first analyzed and characterized based on morphology. Morphological analysis revealed that ADPs have a typical fibroblast-like morphology with an irregular shape, long processes, and oval nuclei containing two or three nucleoli (Fig. 2A). In addition, CFU assay showed that

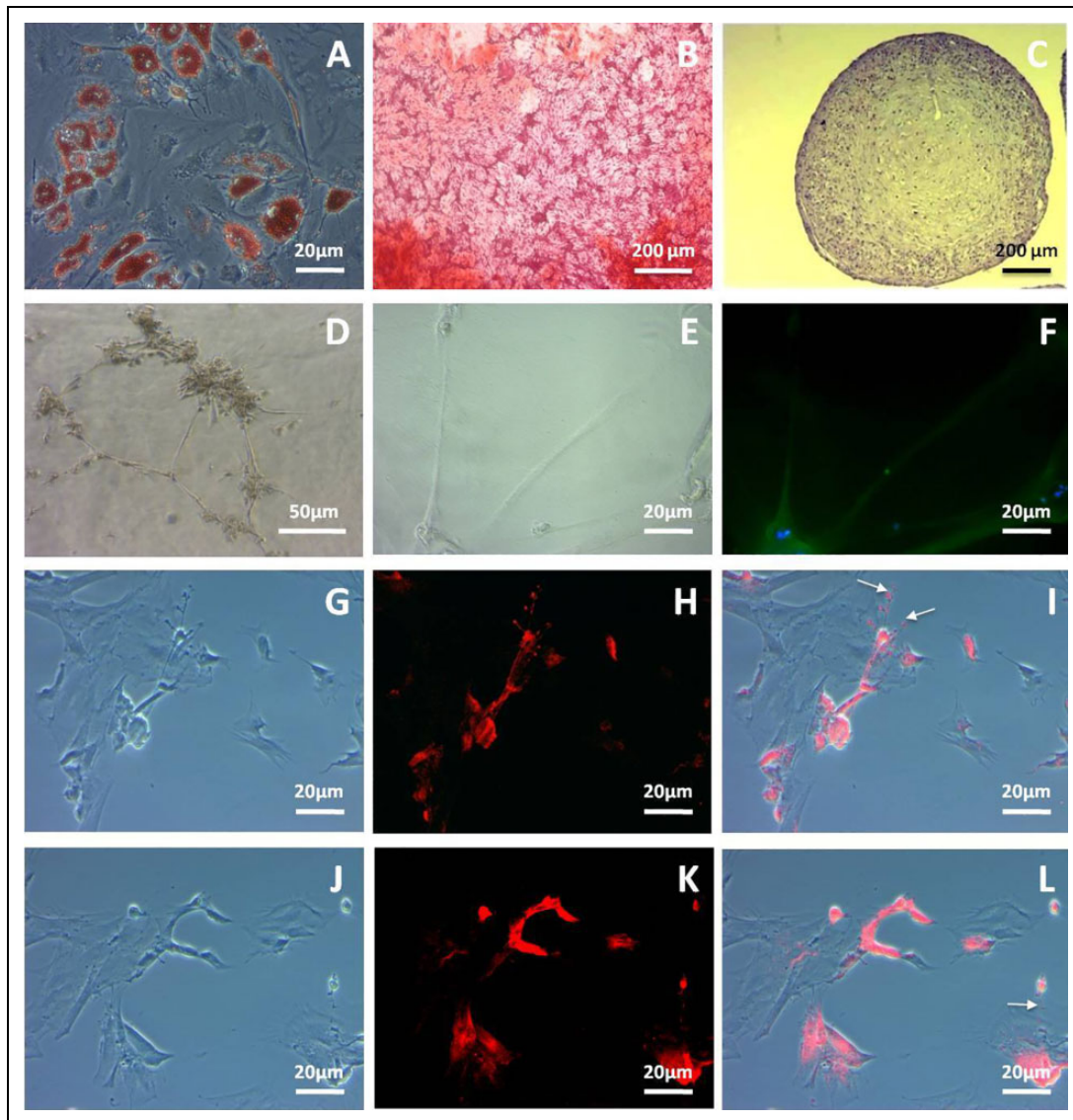


Figure 4. Multilineage *in vitro* differentiation potential of rat ADPs. (A) Adipocytes: red lipid vacuoles stained with Oil Red O. (B) Osteoblasts: alizarin red staining of calcium deposits. (C) Chondrocytes: cartilage matrix staining with toluidine blue. (D–F) Representative images of ADPs after 24 h of endothelial induction. ADPs form capillary-like structures on Matrigel (D, E) and express specific endothelial marker—CD31 (F, green). The nuclei are labeled with DAPI (blue). (G–L) Representative immunofluorescence (red)/phase-contrast images revealed that ADPs differentiated into neuronal-like cells expressing nestin (H, red) and MAP-2 (K, red). (I) Merged image of figures G and H. (L) Merged image of figures J and K. The arrows identify the dendritic-like outgrowths in some neuronal cells. ADPs: adipose-derived pericytes; DAPI: 4',6-diamidino-2-phenylindole.

rat ADPs possess the ability to form clonal fibroblastic colonies (Fig. 2B).

In order to determine a phenotype of rat ADPs, an immunofluorescence analysis was performed. A comprehensive panel of positive and negative CD markers was used to characterize the expression of cell markers (Supplemental Table 1). It was observed that ADPs expressed both pericyte and MSC surface markers such as CD146, NG2, PDGFR- β , CD73, CD90, and CD105. In contrast, the expression of hematopoietic and endothelial markers CD45, CD34, and CD31 in the culture of rat ADPs was not detected (Fig. 3).

To evaluate the multilineage differentiation ability of rat ADPs, five different types of differentiation assays were performed. It was revealed that ADPs can differentiate into adipocytes, chondrocytes, osteoblasts, and endothelial and neuronal cells (Fig. 4). As a result, endothelial differentiation rat ADPs expressed CD31 (a marker of endothelial cells) and formed capillary-like structures on Geltrex matrix. Results on neuroglial differentiation showed that rat ADPs changed their fibroblast-like morphology toward neuronal-like morphology with elongated and dendritic-like outgrowths (Fig. 4G, J). Moreover, immunofluorescence

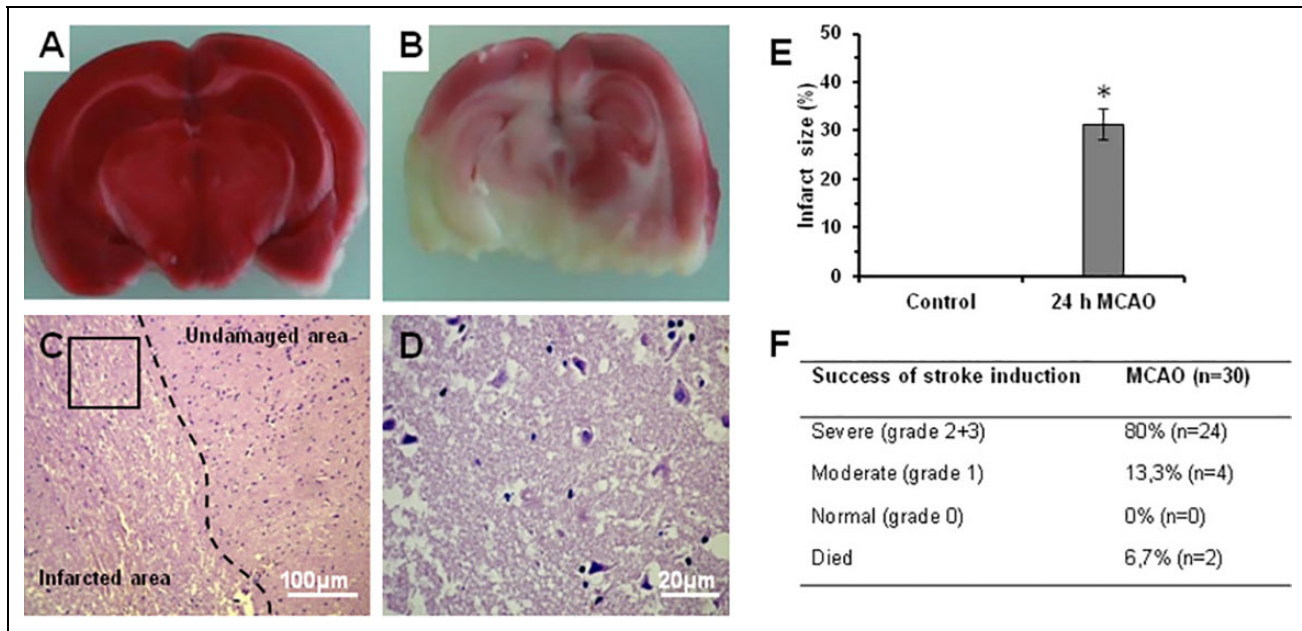


Figure 5. Morphological and histological analysis of rat brain after MCAO. (A) Coronal section of sham-operated rat. (B) Coronal section derived from rat at 24 h after MCAO. TTC staining revealed red undamaged areas and white infarcted areas in the brain. (C) Thin histological section stained by hematoxylin and eosin showing undamaged and infarcted area of the brain. Perivascular and pericellular edema, dystrophy, and degeneration in the infarcted area are seen. The number of neurons is markedly reduced. (D) Magnified image of rectangular area in Fig. 5C showing lesions in the ischemic area. There are cell debris and necrotic neurons with piknotic nuclei. Cytoplasm of neurons is pale and vacuolated. Black arrows identify necrotic and partially lytic forms of neuronal necrosis. White arrows point a pyknotic nucleus amid associated vacuolation of the neuron. (E) Statistics of infarct size. (F) Success of stroke induction after MCAO. * $P < 0.05$ compared with control rats. MCAO: middle cerebral artery occlusion; TTC: 2,3,5-triphenyltetrazolium chloride.

analysis revealed that ADPs expressed markers suitable for neuronal cells such as nestin and MAP2 (Fig. 4H, K).

In order to assess the ischemic stroke, the brain of rats was removed 24 h after MCAO and cut into 2-mm coronal sections (Fig. 5A) and the infarct area was evaluated after staining with TTC. In the sham-control group, TTC staining revealed no lesions in both hemispheres. In contrast, in the MCAO group widespread induction of cerebral infarction in the left hemisphere was observed (Fig. 5B). In comparison to undamaged area, histological study revealed edema, dystrophy, and degeneration of brain tissue in the infarcted area with a number of necrotic neurons containing piknotic nuclei, and pale and vacuolated cytoplasm (Fig. 5C, D). TTC staining showed that the ischemic area accounted for an average $31.4 \pm 3.5\%$ of the total volume at 24 h after MCAO (Fig. 5E). Of 30 rats, 80% had severe functional deficit (<2.5 neurological deficit score), 13.3% had moderate functional deficit, and 6% rats died after MCAO (Fig. 5F). Thus, according to behavior inclusion criteria, in our study we included the rats only with severe neurological deficit. Animals that failed to meet the inclusion criteria did not receive any treatment.

To determine whether the transplanted ADPs could improve neurological function, mNSS and a beam walking test were used. In this study, the following groups of animals have been used: PBS-treated group (control) and three

experimental groups of animals treated different doses of ADPs (1×10^6 , 3×10^6 , and 6×10^6 cells/animal). All rats in the four groups exhibited severe functional deficit on day 1 after MCAO, followed by gradual improvement within the 4-week experimental course. In comparison to the PBS-treated group, experimental animals that received ADPs exhibited significant improvement of neurological function in the beam walking test and mNSS test starting 7 days after treatment (Fig. 6A, B). The maximum therapeutic effect on the recovery of neurological function was detected after transplantation of 3×10^6 and 6×10^6 cells/animal. At the same time, the degree of severity of the sensorimotor deficiency between the two groups was approximately the same. Similar results were obtained after measurement of infarct volume of rat brains at 28 days. H&E staining showed that ADP treatment had decreased lesion volume with respect to the PBS-treated group ($23.98\% \pm 4.04\%$). In particular, it was significantly revealed after administration of 3 mln ADPs ($9.2\% \pm 1.83\%$) and 6 mln ADPs ($8.8\% \pm 1.87\%$) (Fig. 6C, D).

Thus, these data indicate that the improvement of neurological functions observed in the ADP injected groups correlated with less lesion volume in rat brains, which was observed after 4 weeks.

In order to study the effect of transplantation of ADPs on endogenous angiogenesis and neurogenesis in rats after

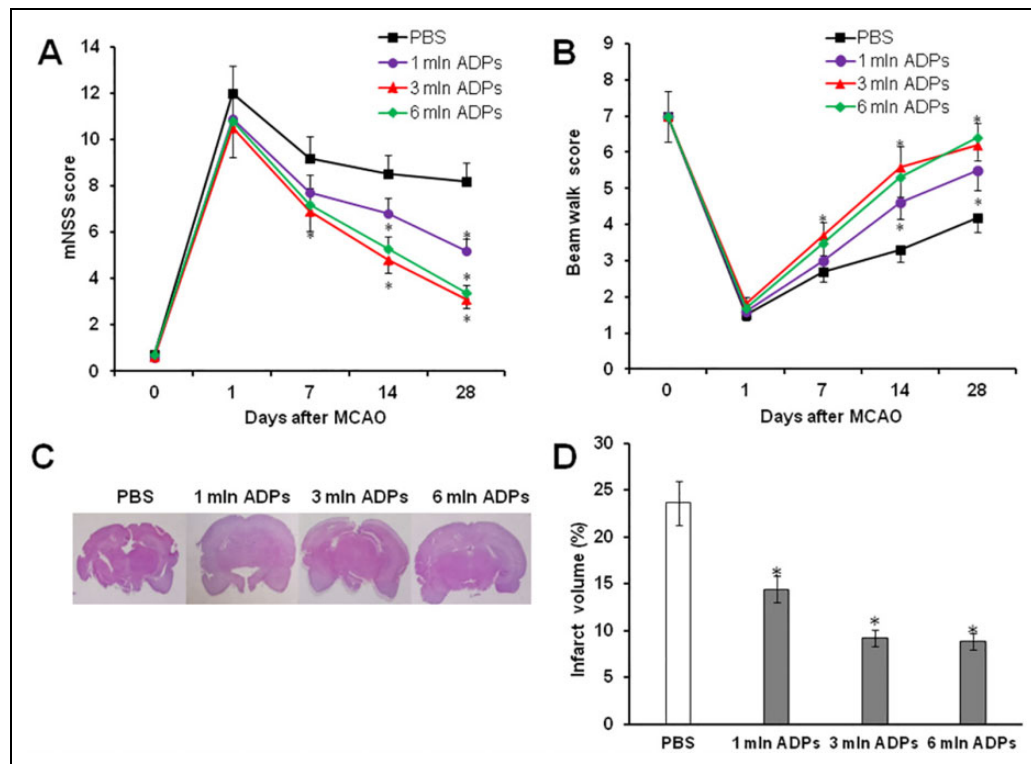


Figure 6. ADP treatment improves neurological outcome and reduces infarct volume in MCAO rats. Neurological performance in mNSS (A) and beam walk test (B) of PBS and ADP-treated rats from 1 to 28 days after MCAO. (C) Representative images of H&E-stained sections of brain infarct lesions at 28 days after PBS and ADP treatment. (D) Quantitative analysis of infarct volume in PBS- and ADP-treated rats at 28 days. * $P < 0.05$ compared with PBS-treated rats, $n = 6$ /group. ADP: adipose-derived pericyte; H&E: hematoxylin and eosin; MCAO: middle cerebral artery occlusion; mNSS: modified neurological severity score; PBS: phosphate-buffered saline.

stroke, an immunohistochemical analysis of ischemic boundary zone (IBZ) of rat brain was then performed using antibodies against CD31 (a marker of endothelial cells), BrdU (a marker of proliferating cells), and DCX (a marker of neuroblasts) (Fig. 7B). It was observed that in comparison to PBS treatment, IV administration of ADPs (3×10^6 and 6×10^6 cells/animal) resulted in a significant increase in the density of microvessels and the percentage of CD31⁺BrdU⁺ proliferating endothelial cells, suggesting that ADPs promote angiogenesis poststroke period (Fig. 7C). Similar treatment effects of ADPs on formation of neuroblasts were observed in the IBZ after stroke. Rats that received IV administration of ADPs (3×10^6 and 6×10^6 cells/animal) demonstrated a significant increase in the percentage of BrdU⁺DCX⁺ neuroblasts in the IBZ (Fig. 7D). Thus, these data suggest that ADPs can promote angiogenesis and neurogenesis in ischemic regions after stroke.

Discussion

In the current study, we first studied the effects of treatment of ischemic stroke with rat ADPs. Our results demonstrate that IV administration of ADPs can significantly improve neurological function after ischemic stroke in rats.

Moreover, our data suggest that enhancement of angiogenesis and neurogenesis in postischemic rat brain may contribute to the underlying therapeutic effect of ADPs.

According to the published data, pericytes represent a unique population of perivascular stem cells that express both pericyte and MSC markers (NG2, α -SMA, CD44, CD146, PDGFR- β , CD73, CD90, CD105, alkaline phosphatase, and vimentin). However, they do not express hematopoietic and endothelial cell markers such as CD34 and CD31^{14,23}. Based on these data, antibodies to CD146, which is a marker of pericytes and endothelial cells, and CD34, a marker of hematopoietic and endothelial cells, were used for the sorting of ADPs. Using FACS, we successfully isolated and characterized CD146⁺CD34⁻ pericytes. Immunocytochemical analysis showed that CD146⁺CD34⁻ pericytes express both pericyte markers CD146, NG2, PDGFR- β , and MSC markers such as CD73, CD90, and CD105. In addition, it was demonstrated that CD146⁺CD34⁻ pericytes, like MSCs, are able to form fibroblastic colonies and differentiate not only to adipocytes, chondrocytes, and osteoblasts, but also to endothelial-like cells and neuronal cells. These results suggest that isolated ADPs have a high multipotent potential and may promote functional recovery after stroke through enhancement of angiogenesis and neurogenesis in the damaged brain.

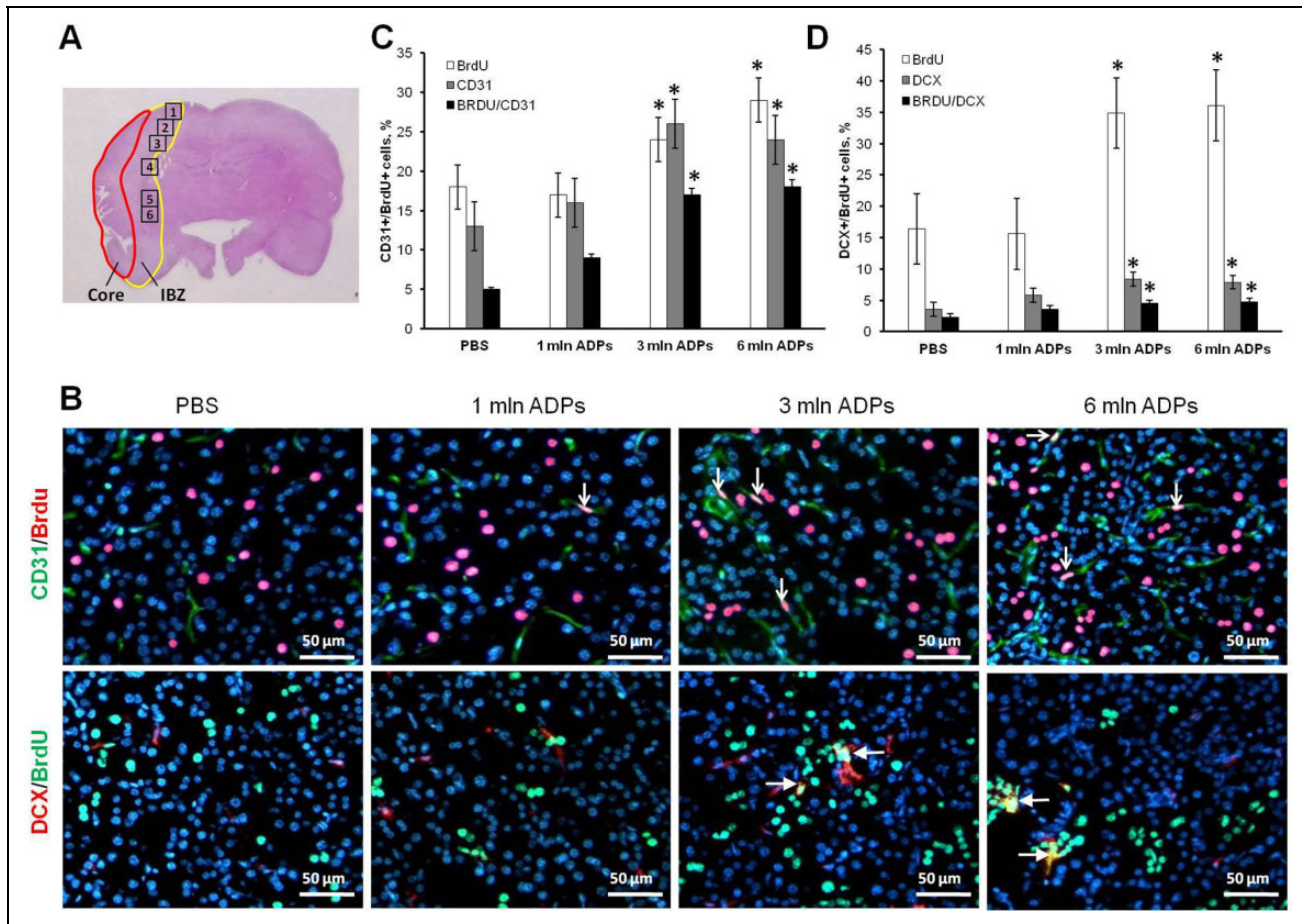


Figure 7. ADPs increase neurogenesis and angiogenesis in the IBZ. (A) Schematic figure showing six areas (three from the cortex, two from the striatum, and one from the corpus callosum) selected along the IBZ. (B) Representative merged images show the double-stained cells with CD31 and BrdU or doublecortin (DCX) and BrdU. The nuclei are stained with DAPI. White arrows indicate proliferating BrdU+CD31+ endothelial cells. White arrows point proliferating BrdU+DCX+ neuroblasts. (C) The diagram shows the percentage of BrdU+CD31+ endothelial cells. (D) The percentage of BrdU+/DCX+ cells in the IBZ. Compared with PBS treatment, IV administration of ADPs (3 mln and 6 mln) significantly increased a density of microvessels and the percentage of neuroblasts in the IBZ in ischemic stroke rats at 28 days. * $P < 0.05$ compared with PBS-treated rats, $n = 6$ /group. ADPs: adipose-derived pericytes; BrdU: 5-bromodeoxyuridine; DAPI: 4',6-diamidino-2-phenylindole; IBZ: ischemic boundary zone; IV: intravenous; PBS: phosphate-buffered saline.

In order to examine whether a single transplantation of allogeneic ADPs could enhance recovery of neurological function after ischemic stroke, we used three different doses: 1×10^6 , 3×10^6 , and 6×10^6 ADPs. Here, we have found that IV administration of ADPs (especially at 3×10^6 and 6×10^6 cells/animal) significantly improved the neurological outcome and reduced infarct lesion after stroke compared to PBS treatment. However, it is interesting to note that the effects observed after administration of 3×10^6 and 6×10^6 ADPs were approximately the same. Accumulating evidence has suggested that transplantation of pericytes can promote endogenous angiogenesis and neurogenesis to improve neurological function of damaged brain after ischemic stroke²⁸. Our immunohistochemical analysis showed that the administration of ADPs markedly enhanced both angiogenesis and neurogenesis in the border zone of ischemic injury, which led to an increase of vascular density

(CD31-positive cells) and in the number of proliferating neuroblasts (DCX-positive cells). Similar data were obtained by Tsai et al. who demonstrated that bone marrow MSCs substantially increased neuronal progenitor cells surrounding lateral ventricle in a stroke-affected hemisphere²⁹. Other researchers showed that the promotion of angiogenesis and neurogenesis in the injured brain of animals with stroke is mediated by MSC exosomes and the actions of their miRNA content. In addition, the mechanisms underlying the beneficial effects of *in vivo* MSC and cell-free exosome treatments showed similar results³⁰.

What are the mechanisms that promote neurological function and regeneration of damaged brain with pericyte transplantation after ischemic stroke? Based on the published data, we suggest that therapeutic effects of pericytes mainly exert through paracrine mechanism. This is justified by the fact that the barrier function of the blood-brain barrier may

prevent the penetration of pericytes into the ischemic sites of brain³¹. Thus, transplanted pericytes may not directly interact with cells of injured microenvironment and differentiate into different neurovascular cells to reconstruct neurovascular units under pathological conditions. Pericytes secrete multiple paracrine growth factors and cytokines, which stimulate different cell types involved in tissue repair^{32,33}. They produce a variety of neurotrophic factors such as glial cell line-derived neurotrophic factor, brain-derived neurotrophic factor, nerve growth factor, and neurotrophin-3, which facilitate neuronal and axonal regeneration as well as contribute to neuronal survival^{34,35}. In addition to secretion of neurotrophic factors, pericytes also produce angiogenic factors such as vascular endothelial growth factor (VEGF), basic fibroblast growth factor, and angiopoietin-1. VEGF stimulates proliferation of endothelial cells and preserves their functions in the ischemic brain. It has been shown that IV administration of recombinant VEGF before MCAO significantly enhanced capillary density, reduced lesion volume, and inflammation in animals with stroke³⁶. In addition, Chen et al. reported that cultured pericytes can produce heparin binding epidermal growth factor, basic fibroblast growth factor, and keratinocyte growth factor in higher amount than in those of regular MSCs³². All these growth factors are well known to significantly promote tissue regeneration.

Thus, promotion of neurological function by IV administration of ADPs may be due to the production of paracrine growth factors by ADPs.

Conclusion

In conclusion, results shown in the current study indicate that treatment of ischemic stroke with ADPs can significantly improve the neurological status and promote endogenous angiogenesis and neurogenesis. Thus, ADPs are a promising candidate for the development of a novel treatment for ischemic stroke.

Acknowledgments

We thank Mr. Yeldar Baiken (Nazarbayev University) for his help in a cell sorting experiment.

Ethical Approval

The experimental protocols were approved by the Local Ethics Committee of National Center for Biotechnology.

Statement of Human and Animal Rights

All animal studies were approved by the Local Ethics Committee of National Center for Biotechnology and were performed according to Good Laboratory Practice.

Statement of Informed Consent

There are no human subjects in this article and informed consent is not applicable.


Declaration of Conflicting Interests


The author(s) declared no potential conflicts of interest with respect to the research, authorship, and/or publication of this article.

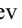
Funding

The author(s) disclosed receipt of the following financial support for the research, authorship, and/or publication of this article: This work was financially supported by Ministry of Education and Science of the Republic of Kazakhstan (Grants AP05134447 and 4131/GF4).

ORCID iDs

Vyacheslav Ogay  <https://orcid.org/0000-0001-5029-5255>

Sholpan Askarova  <https://orcid.org/0000-0001-6161-1671>

Berik Zhetpisbayev  <https://orcid.org/0000-0002-7068-7827>

Supplemental Material

Supplemental material for this article is available online.

References

1. Donnan GA, Fisher M, Macleod M, Davis SM. Stroke. *Lancet*. 2008;371(9624):1612–1623.
2. Thrift AG, Cadilhac DA, Thayabaranathan T, Howard G, Howard VJ, Rothwell PM, Donnan GA. Global stroke statistics. *Int J Stroke*. 2014;9(1):6–18.
3. Lees KR, Bluhmki E, von Kummer R, Brott TG, Toni D, Grotta JC, Albers GW, Kaste M, Marler JR, Hamilton SA, Tilley BC, et al. Time to treatment with intravenous alteplase and outcome in stroke: an updated pooled analysis of ECASS, ATLANTIS, NINDS, and EPITHET trials. *Lancet*. 2010;375(9727):1695–1703.
4. Cronin CA. Intravenous tissue plasminogen activator for stroke: a review of the ECASS III results in relation to prior clinical trials. *J Emerg Med*. 2010;38(1):99–105.
5. IST-3 collaborative group, Sandercock P, Wardlaw JM, Lindley RI, Dennis M, Cohen G, Murray G, Innes K, Venables G, Czlonkowska A, Kobayashi A, et al. The benefits and harms of intravenous thrombolysis with recombinant tissue plasminogen activator within 6 h of acute ischemic stroke (the third international stroke trial [IST-3]): a randomized controlled trial. *Lancet*. 2012;379(9834):2352–2363.
6. Kalladka D, Muir KW. Brain repair: cell therapy in stroke. *Stem Cells Cloning*. 2014;7:31–44.
7. Hao L, Zou Z, Tian H, Zhang Y, Zhou H, Liu L. Stem cell-based therapies for ischemic stroke. *Biomed Res Int*. 2014;2014:468748.
8. Dulamea AO. The potential use of mesenchymal stem cells in stroke therapy - From bench to bedside. *J Neurol Sci*. 2015;352(1–2):1–11.
9. Gutiérrez-Fernández M, Rodríguez-Frutos B, Otero-Ortega L, Ramos-Cejudo J, Fuentes B, Díez-Tejedor E. Adipose tissue-derived stem cells in stroke treatment: from bench to bedside. *Discov Med*. 2013;16(86):37–43.
10. Gutiérrez-Fernández M, Rodríguez-Frutos B., Ramos-Cejudo J, Teresa Vallejo-Cremades M, Fuentes B, Cerdán S, Díez-Tejedor E. Effects of intravenous administration of allogenic

- bone marrow and adipose tissue-derived mesenchymal stem cells on functional recovery and brain repair markers in experimental ischemic stroke. *Stem Cell Res Ther.* 2013;4(1):11.
11. Cathery W, Faulkner A, Maselli D, Madeddu P. Concise review: the regenerative journey of pericytes towards clinical translation. *Stem Cells.* 2018;36(9):1295–1310.
 12. Harrell CR, Simovic Markovic B, Fellabaum C, Arsenijevic A, Djonov V, Volarevic V. Molecular mechanisms underlying therapeutic potential of pericytes. *J Biomed Sci.* 2018;25(1):21.
 13. Lamagna C, Bergers G. The bone marrow constitutes a reservoir of pericyte progenitors. *J Leukoc Biol.* 2006;80(4):677–681.
 14. Crisan M, Yap S, Casteilla L, Chen CW, Corselli M, Park TS, Andriolo G, Sun B, Zheng B, Zhang L, Norotte C, et al. A perivascular origin for mesenchymal stem cells in multiple human organs. *Cell Stem Cell.* 2008;3(3):301–313.
 15. Nakagomi T, Kubo S, Nakano-Doi A, Sakuma R, Lu S, Narita A, Kawahara M, Taguchi A, Matsuyama T. Brain vascular pericytes following ischemia have multipotential stem cell activity to differentiate into neural and vascular lineage cells. *Stem Cells.* 2015;33(6):1962–1974.
 16. Farrington-Rock C, Crofts NJ, Doherty MJ, Ashton BA, Griffin-Jones C, Canfield AE. Chondrogenic and adipogenic potential of microvascular pericytes. *Circulation.* 2004;110(15):2226–2232.
 17. Montiel-Eulefi E, Nery AA, Rodrigues LC, Sánchez R, Romero F, Ulrich H. Neural differentiation of rat aorta pericyte cells. *Cytometry A.* 2012;81(1):65–71.
 18. Dore-Duffy P, Katychev A, Wang X, Van Buren E. CNS microvascular pericytes exhibit multipotential stem cell activity. *J Cereb Blood Flow Metab.* 2006;26(5):613–624.
 19. Ishitsuka K, Ago T, Arimura K, Nakamura K, Tokami H, Maki-hara N, Kuroda J, Kamouchi M, Kitazono T. Neurotrophin production in brain pericytes during hypoxia: a role of pericytes for neuroprotection. *Microvascular Res.* 2012;83(3):352–359.
 20. Yamashima T, Tonchev AB, Vachkov IH, Popivanova BK, Seki T, Sawamoto K, Okano H. Vascular adventitia generates neuronal progenitors in the monkey hippocampus after ischemia. *Hippocampus.* 2004;14(7):861–875.
 21. Dar A, Domev H, Ben-Yosef O, Tzukerman M, Zeevi-Levin N, Novak A, Germanguz I, Amit M, Itskovitz-Eldor J. Multipotent vasculogenic pericytes from human pluripotent stem cells promote recovery of murine ischemic limb. *Circulation.* 2012;125(1):87–99.
 22. Chen CW, Okada M, Proto JD, Gao X, Sekiya N, Beckman SA, Corselli M, Crisan M, Saparov A, Tobita K, Péault B, et al. Human pericytes for ischemic heart repair. *Stem Cells.* 2013;31(2):305–316.
 23. Crisan M, Corselli M, Chen WC, Péault B. Perivascular cells for regenerative medicine. *J Cell Mol Med.* 2012;16(12):2851–2860.
 24. Uluç K, Miranpuri A, Kujoth GC, Aktüre E, Başkaya MK. Focal cerebral ischemia model by endovascular suture occlusion of the middle cerebral artery in the rat. *J Vis Exp.* 2011;(48):1978.
 25. Bederson JB, Pitts LH, Tsuji M, Nishimura MC, Davis RL, Bartkowski H. Rat middle cerebral artery occlusion: evaluation of the model and development of a neurologic examination. *Stroke.* 1986;17(3):472–476.
 26. Goldstein LB, Davis JN. Beam-walking in rats: studies towards developing an animal model of functional recovery after brain injury. *J Neurosci Methods.* 1990;31(2):101–107.
 27. Swanson RA, Morton MT, Tsao-Wu G, Savalos RA, Davidson C, Sharp FR. A semiautomated method for measuring brain infarct volume. *J Cereb Blood Flow Metab.* 1990;10(2):290–293.
 28. Cheng J, Korte N, Nortley R, Sethi H, Tang Y, Attwell D. Targeting pericytes for therapeutic approaches to neurological disorders. *Acta Neuropathol.* 2018;136(4):507–523.
 29. Tsai MJ, Tsai SK, Hu BR, Liou DY, Huang SL, Huang MC, Huang WC, Cheng H, Huang SS. Recovery of neurological function of ischemic stroke by application of conditioned medium of bone marrow mesenchymal stem cells derived from normal and cerebral ischemia rats. *J Biomed Sci.* 2014;21(1):5.
 30. Xin H, Li Y, Cui Y, Yang JJ, Zhang ZG, Chopp M. Systemic administration of exosomes released from mesenchymal stromal cells promote functional recovery and neurovascular plasticity after stroke in rats. *J Cereb Blood Flow Metab.* 2013;33(11):1711–1715.
 31. Cai W, Liu H, Zhao J, Chen LY, Chen J, Lu Z, Hu X. Pericytes in brain injury and repair after ischemic stroke. *Transl Stroke Res.* 2017;8(2):107–121.
 32. Chen CW, Montelatici E, Crisan M, Corselli M, Huard J, Laz-zari L, Péault B. Perivascular multi-lineage progenitor cells in human organs: regenerative units, cytokine sources or both? *Cytokine Growth Factor Rev.* 2009;20(5–6):429–434.
 33. Mansurov N, Chen WCW, Awada H, Huard J, Wang Y, Saparov A. A controlled release system for simultaneous delivery of three human perivascular stem cell-derived factors for tissue repair and regeneration. *J Tissue Eng Regen Med.* 2018;12(2):e11164–e11172.
 34. Shimizu F, Sano Y, Saito K, Abe MA, Maeda T, Haruki H, Kanda T. Pericyte-derived glial cell line-derived neurotrophic factor increase the expression of claudin-5 in the blood-brain barrier and the blood-nerve barrier. *Neurochem Res.* 2012;37(2):401–409.
 35. Arimura K, Ago T, Kamouchi M, Nakamura K, Ishitsuka K, Kuroda J, Sugimori H, Ooboshi H, Sasaki T, Kitazono T. PDGF receptor beta signaling in pericytes following ischemic brain injury. *Curr Neurovasc Res.* 2012;9(1):1–9.
 36. Zechariah A, ElAli A, Doepfner TR, Jin F, Hasan MR, Helfrich I, Mies G, Hermann DM. Vascular endothelial growth factor promotes pericyte coverage of brain capillaries, improves cerebral blood flow during subsequent focal cerebral ischemia, and preserves the metabolic penumbra. *Stroke.* 2013;44(6):1690–1697.